ACS Catalysis

Research Article

pubs.acs.org/acscatalysis

Computational Mechanistic Study of Fe-Catalyzed Hydrogenation of Esters to Alcohols: Improving Catalysis by Accelerating Precatalyst Activation with a Lewis Base

Shuanglin Qu,[†] Huiguang Dai,[‡] Yanfeng Dang,[†] Chunyu Song,[†] Zhi-Xiang Wang,*[,†,§] and Hairong Guan*[,‡]

[†]School of Chemistry and Chemical Engineering, University of the Chinese Academy of Sciences, Beijing,100049, China

[‡]Department of Chemistry, University of Cincinnati, P.O. Box 210172, Cincinnati, Ohio 45221-0172, United States

[§]Collaborative Innovation Center of Chemical Science and Engineering, Tianjin, 300072, China

Supporting Information

ABSTRACT: DFT calculations have been performed to gain mechanistic insight into ester hydrogenation to alcohols (exemplified by $PhCO_2CH_3$ +2H_2 → $PhCH_2OH$ + CH_3OH), catalyzed by a well-defined Fe-PNP pincer hydridoborohydride complex (**1**). The entire catalytic process includes precatalyst activation to an active species *trans*-dihydride complex **2**, **2**-catalyzed transformation of $PhCO_2CH_3$ + H_2 → PhCHO + CH_3OH, hydrogenation of PhCHO to $PhCH_2OH$, and catalyst regeneration via H_2 addition to the dehydrogenated **2** (i.e., complex **5**). The transformation, $PhCO_2CH_3$ + H_2 → PhCHO + CH_3OH, proceeds via hydrogenation of $PhCO_2CH_3$ to a hemiacetal $PhCH(OH)(OCH_3)$, followed by decomposition of the hemiacetal to methanol and benzaldehyde. The Fe-complex **5** was found to be capable of facilitating the decomposition of the hemiacetal. The ineffectiveness of the catalytic system in hydrogenating methyl salicylate is attributed to the intrinsically lower reactivity of the ester toward C═O reduction and a very facile side-reaction, which is adding the phenol OH group of the hemiacetal intermediate stemmed from methyl salicylate to the Fe−N active site of **5**. Computations of various catalyst initiation pathways show that the initiation without the aid of an additive is very unfavorable, thus we suggest the use of a Lewis base such as NR_3 (R = Me and Et) and PR_3 (R = ^{n}Bu and ^{t}Bu) to accelerate precatalyst (**1**) activation, because a Lewis base could form a stable adduct (BH_3−NR_3/PR_3) with the BH_3 moiety of **1**. In agreement with greatly enhanced kinetics and thermodynamics of the initiation process suggested by the DFT calculations, experimental study shows that the addition of a catalytic amount of NEt_3 doubled the yield of benzyl alcohol from the hydrogenation of methyl benzoate, when compared to the case without using any additive. The *trans* effect of the hydride on the reactivity of **2** and steric effect of the pincer substituents on the stability of **2** are also discussed.

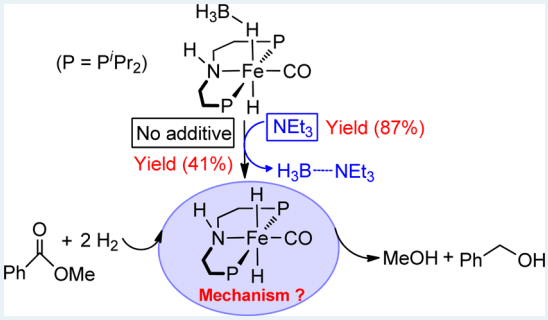

KEYWORDS: *iron catalysis, hydrogenation of esters, mechanism, catalyst initiation, Lewis base, DFT calculations*

1. INTRODUCTION

Hydrogenation of esters to alcohols constitutes an important class of chemical transformations[1] for the synthesis of natural products and organic building blocks. In industry, this process is widely used to manufacture agrochemicals, pharmaceuticals, flavors, and fragrances.[2,3] Traditional laboratory approaches using stoichiometric amounts of metal hydride reductants (e.g., $LiAlH_4$ and $NaBH_4$) suffer from poor compatibility with functional groups, low atom economy, and concerns with respect to copious amounts of wastes.[4] Industrial methods employing heterogeneous catalysts for hydrogenation of esters to alcohols are, however, energy intensive due to high temperature and pressure required for the reactions.[5] In that regard, there is a growing demand for the development of homogeneous catalytic systems for ester reduction, because of their potential to operate under milder conditions with tolerance to a broader range of functional groups.

In the past few decades, Ru- and Os-based homogeneous catalysts have been developed for ester hydrogenation.[6] The catalysts reported prior to the early 2000s were often limited to hydrogenating activated esters such as dimethyl oxalate[7] and fluorinated esters,[8] while hydrogenation of nonactivated esters still required high temperature and high H_2 pressure.[9] Significant progresses were made around 2006 by Milstein et al.[10] and Firmenich SA[11] who developed Ru-based catalysts for hydrogenation of nonactivated esters under relatively mild conditions. Since then, many other Ru- and Os-based catalysts

Received: July 28, 2014
Revised: October 10, 2014
Published: October 24, 2014

   dx.doi.org/10.1021/cs501089h | ACS Catal. 2014, 4, 4377−4388

Scheme 1. Three Pathways for Hydrogenation of Alkyl Formate to Formaldehyde and Alcohol Catalyzed by a PNN-Ru Pincer Complex

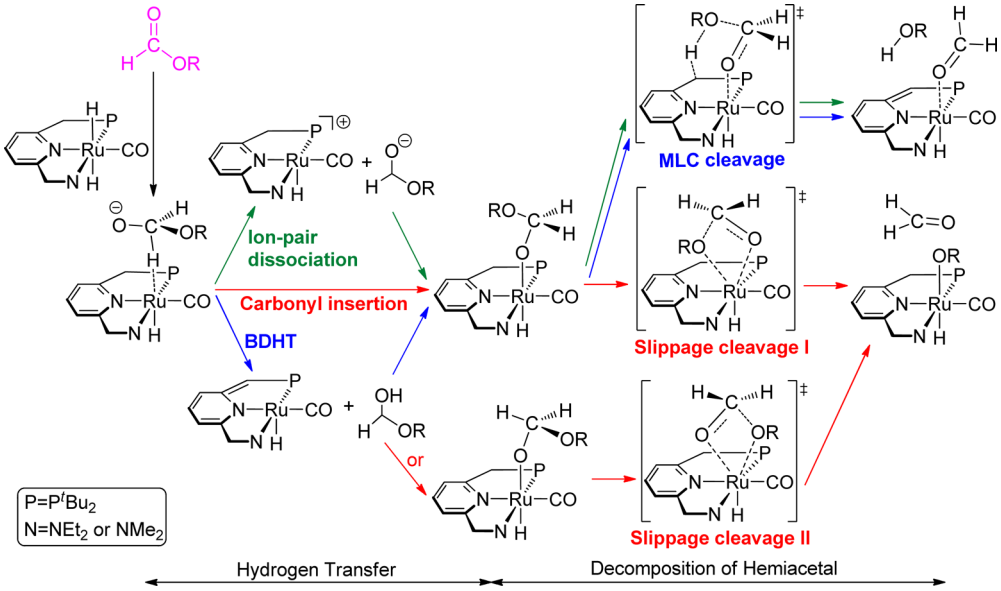

have been prepared to improve the efficiency of ester hydrogenation.[1b,12] The escalating costs of precious metals have prompted chemists to search new catalysts based on iron, which is inexpensive, earth-abundant, and nontoxic. In early 2014, Milstein et al. reported the first Fe-based catalyst for the hydrogenation of activated fluorinated esters with the aid of a base such as KO^{t}Bu.[13] More recently, the Guan[14] and Beller groups[15] independently developed a catalytic system using a well-defined Fe-PNP pincer hydridoborohydride complex (**1**) as a precatalyst for the reduction of a wide range of nonactivated esters. These catalytic reactions operate under relatively mild conditions (10−30 atm H_2, 100−135 °C) without using any additives (eq 1, below). It is noted that the Fe-complex (**1**) and its analogues have been applied for dehydrogenations of alcohols[16] and formic acid,[17] ketone hydrogenation,[18] and hydrogenation/dehydrogenation of N-heterocycles.[19]

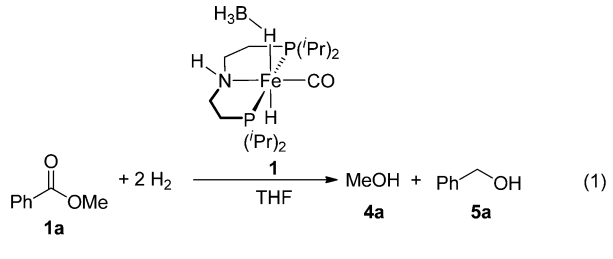

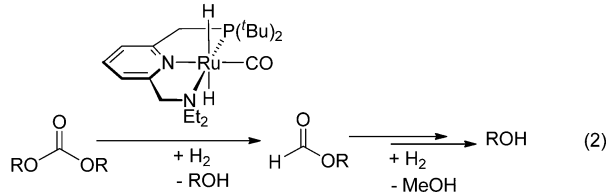

To further improve the Fe-based catalytic system, it is of importance to understand the mechanistic details of the catalytic process as a whole. It should be mentioned that Beller et al. reported a brief computational mechanistic study in their original report.[15] For a deeper understanding of the system, we decided to perform a more thorough mechanistic study that can guide our future experimental studies. The present work mainly focuses on three aspects. First, catalyst initiation often plays a crucial role in determining the performance of a catalytic system. Beller et al. proposed that the catalyst initiation could take place via formation of B_2H_6 from **1**. We explored other possibilities, on the basis of which, we computationally predicted and experimentally verified a strategy to facilitate the initiation process, thus enhancing the catalytic efficiency of the system. Second, we have previously computed the catalytic mechanism[20] (the blue pathway in Scheme 1) of PNN-Ru catalyzed carbonate hydrogenation which was developed by Milstein et al. (eq 2).[21] Yang[22] and Hasanayn[23] also independently performed computational mechanistic studies of the transformation and reported different preferred pathways, as illustrated in Scheme 1 (the green pathway by Yang and the red pathway by Hasanayn). In principle, ester hydrogenation is similar to the hydrogenation of alkyl formate described in eq 2. Beller et al. examined the reaction pathway[15] that is similar to ours for carbonate hydrogenation, but it is unclear if the mechanisms proposed by Yang and Hasanayn are energetically more favorable. We are interested in identifying which pathway among the three is more favorable in the present catalytic system (eq 1). In addition, although Beller et al. suggested that the decomposition of hemiacetal intermediate takes place without the involvement of the iron complex, the present study shows a Fe-based intermediate greatly facilitates the decomposition. Finally, in our experimental study, we observed that the Fe-PNP complex **1** was effective for various esters but failed for methyl salicylate. We are particularly curious about the causes, which could help understand the catalytic system more deeply.

2. COMPUTATIONAL AND EXPERIMENTAL DETAILS

Computational Details. Actual structures of the catalyst and substrates rather than simplified models were calculated in this study. All substrates and Fe-complexes were optimized at B3LYP[24]/6-31G(d,p)[25] level in the gas phase. The basis set SDD was used for the Ru atom. Harmonic frequency analysis calculations were subsequently performed to verify the

dx.doi.org/10.1021/cs501089h | ACS Catal. 2014, 4, 4377−4388

Scheme 2. Energetics for Various Catalyst Initiations by Trapping BH_3

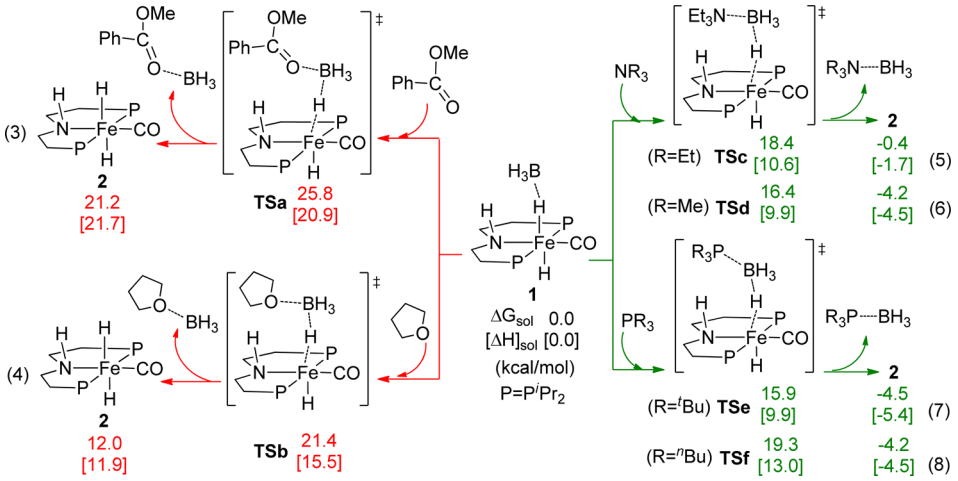

optimized structures to be minima (no imaginary frequency) or transition states (TSs, having unique one imaginary frequency). The energies were then improved by M06[26]/6-311++G-(d,p)[27]//B3LYP/6-31G(d,p) single-point calculations with solvent effects accounted by the SMD[28] solvent model, using the experimental solvent (THF). The combined use of the two DFT functionals has been successfully applied to account for various transition-metal-catalyzed reactions.[29] The refined energies were then corrected to enthalpies and free energies at 298.15 K and 1 atm, using the gas phase B3LYP/6-31G(d,p) harmonic frequencies. It should be emphasized that such thermal corrections based on the ideal gas phase model inevitably overestimate entropy contributions to free energies for reactions in solvent, in particular for reactions involving multicomponent change, because of ignoring the suppressing effect of solvent on the rotational and transitional freedoms of substrates. The entropy overestimation by ideal gas phase model was also demonstrated by experimental studies.[30,31] Because no standard quantum mechanics-based approach is available to accurately calculate entropy in solution, we adopted the approximate approach proposed by Martin et al.[32] According to their approach, a correction of 4.3 kcal/mol applies to per component change for a reaction at 298.15 K and 1 atm (i.e., a reaction from *m*- to *n*-components has an additional correction of $(n - m) \times 4.3$ kcal/mol). Previously, we applied the correction protocol for mechanistic studies of various catalytic reactions and found such corrected free energies were more reasonable than enthalpies and uncorrected free energies,[33] although the protocol is by no means accurate. In the following, *we discuss the mechanism in terms of the corrected free energies and give the enthalpies for references in the brackets in the relevant* figures. All calculations were carried out using Gaussian 09 program.[34] Total energies and Cartesian coordinates of all optimized structures are given in Supporting Information (SI).

Experimental Details. In a glovebox, complex **1** (10 mg, 25 μmol), Et_3N (11.6 μL, 83 μmol), and methyl benzoate (105 μL, 833 μmol) were mixed with 0.5 mL of toluene in a small test tube, which was placed in a HEL CAT18 high-pressure vessel. The vessel was sealed, flushed with H_2 three times, and placed under 150 psig of H_2 pressure. The vessel was then heated by a 60 °C oil bath for 3 h. Upon cooling, H_2 was vented and tridecane (80 μL, 328 μmol, internal standard) was added to the test tube. A small aliquot was withdrawn from the test tube, diluted with approximately 4 mL of ethyl acetate, and filtered through a short pad of silica gel prior to GC analysis. The percentage conversion and the percentage yield of benzyl alcohol were calculated by comparing the integrations of methyl benzoate and benzyl alcohol with that of the internal standard.

3. RESULTS AND DISCUSSION

The Fe-PNP complex (**1**) was applied to hydrogenate various esters.[14,15] Beller et al. chose methyl benzoate **1a** (eq 1) as a representative substrate to compute the mechanism. We used the same transformation in our mechanistic investigation. Frequently, a catalytic transformation includes activation of the catalyst precursor to an active species and the reaction catalyzed by the active species. For the present catalytic system, experimental studies[14,15] have suggested that **1** is a catalyst precursor and **2** (see Scheme 2) is the actual catalyst to perform catalysis. However, it is unclear how **2** was generated under the catalytic condition. In the following sections, we first discuss how **1** is activated to yield **2** (section 3.1) and then how **2** catalyzes the subsequent ester hydrogenation (section 3.2). In section 3.3, we provide the mechanistic insight on why the catalyst was not able to hydrogenate methyl salicylate **6a**.

3.1. Conversion of 1 to the Active Catalyst 2. In both experimental studies, no additive was used for the hydrogenation. Here we compare the energetics of possible pathways for catalyst initiation.

The activation of **1** via direct dissociation of BH_3 is endergonic by 26.8 kcal/mol without a transition state, as indicated by the scanned potential energy surface (PES) of the dissociation (see Figure S1). Compared to the direct BH_3 dissociation, the process ($2 \times \mathbf{1} \rightarrow 2 \times \mathbf{2} + B_2H_6$) proposed by Beller et al. only slightly enhances the thermodynamics by 1.8 kcal/mol (see eq 2 in Figure S1).

Because the substrate (**1a**) and the solvent THF feature a Lewis basic O-center, we explored if the activation of **1** to **2** could be facilitated by forming Lewis acid/base adducts between BH_3 of **1** and **1a** or THF. However, due to the weak electron-donating nature of the O-centered Lewis bases, the initiations via eq 3 and 4 (Scheme 2) are also endergonic by 21.2 and 12.0 kcal/mol, respectively, and need to cross barriers of 25.8 and 21.4 kcal/mol, respectively. Consistent with the energetic results of eq 4, Jones et al. recently observed the reverse reaction of eq 4 in C_6D_6.[19] Considering the temperature

dx.doi.org/10.1021/cs501089h | ACS Catal. 2014, 4, 4377−4388

Table 1. Catalytic Hydrogenation of Methyl Benzoate in Toluene with or without an Additive

catalyst	additive	P (H_2)	temp/time	conversion/yield[a]
1 (3 mol %)	NEt_3 (10 mol %)	150 psig	60 °C/3h	95%/87%
1 (3 mol %)	none	150 psig	60 °C/3h	48%/41%

[a]Conversion of **1a** and yield of **5a** were determined by GC.

(100−135 °C) applied experimentally, the energetic results indicate that **2** could be kinetically accessible via microscopic equilibriums of eq 3 and 4. Nevertheless, we reasoned there must be another factor to drive the formation of **2**. Once the BH_3 moiety dissociates from **1**, the species could dimerize to B_2H_6 which can further undergo chain reactions to give more stable higher boranes (e.g., B_5H_{11})[35] at elevated temperature. The dimerization of BH_3 is exergonic by 28.7 kcal/mol and the formation of B_5H_{11} is exergonic by 61.0 kcal/mol (see Scheme S1). Thus, as B_2H_6 and higher boranes (e.g., B_5H_{11}) are formed, the conversion of **2** + BH_3 to **1** would not proceed despite the fact that it is kinetically and thermodynamically feasible, because there is no BH_3 source available in the system due to the formation of more stable higher boranes. It should be emphasized that this initiation process does not necessarily need to reverse the unfavorable thermodynamics of transformation from **1** to **2**. For example, our calculations show that the transformation (**1** → **2** + 1/5*B_5H_{11} + 2/5*H_2) is still endergonic by 14.7 kcal/mol (see Scheme S1). This value is less than direct dissociation energy of BH_3 from **1** (26.8 kcal/mol), thus improving the transformation thermodynamically. To some extent, this initiation process is analogous to catalytic acceptorless dehydrogenations of alcohols or alkanes,[36] which are substantially endergonic but can take place because of releasing H_2 gas. In addition, we further confirmed that **1** is not able to promote the reaction without releasing BH_3 moiety (see Figure S2). On the basis of experimental observations and our above analyses, we believe that **2** is the actual catalyst for these transformations.

Under the experimental conditions (without adding any additives), the energetic results for the catalyst initiation suggest that the hydrogenation process is hampered by BH_3 dissociation, but at the same time, the results point out potential solutions to improving the catalytic performance of the system. Thus, we hypothesized that a stronger Lewis base may accelerate the initiation process. Indeed, If a stronger Lewis base such as NR_3 (R = Et (eq 5)/Me (eq 6)) is applied, the formation of the more stable BH_3NR_3 adduct drives the initiation kinetically and thermodynamically; the barrier is 18.4/16.4 kcal/mol, and the process now becomes exergonic by 0.4/4.2 kcal/mol. The Lewis base PR_3(R = ^{t}Bu (eq 7)/^{n}Bu (eq 8)) should also be effective to activate the catalyst precursor according to the computed kinetics and thermodynamics. Furthermore, the energetic results ($\Delta G^{\ddagger}$ = 19.3 and ΔG = −4.2 kcal/mol) of eq 8 agree with our experimental observation that **2** could be formed facilely when one equiv of P^nBu_3 was introduced in the solution of **1**.[14] The energetic results show that the stronger Lewis bases may promote the catalyst activation. However, because the species generated after hydrogen transfer from **2** to an ester (i.e., **5**, see below in Scheme 3) possesses a Lewis acidic Fe center, we further probed if the Lewis base additives form stable Lewis acid−base adducts with **5** to inhibit the catalysis. Relative to **5** + additive, the complexation energies of the additives with **5** are 2.4 (NEt_3), 2.1 (NMe_3), 1.1 (P^tBu_3), and 4.0 (P^nBu_3) kcal/mol, respectively (see SI), indicating the additives could facilitate the generation of the active catalyst without negatively impacting the activity of the active catalyst.

The above computational results (eqs 5−8) prompted us to test if a Lewis base (e.g., NEt_3) is able to promote the generation of **2**, thus improving the performance of the catalytic system. To support the computational prediction, we added a catalytic amount of NEt_3 to perform the same reaction shown in eq 1. The results are given in Table 1. Compared to the reaction without an additive,[37] the addition of the Lewis base does increase the catalytic activity of the system.

3.2. Catalytic Mechanism. The active species **2** generated from **1** catalyzes the transformation of $PhCO_2CH_3$ + $2H_2$ → $PhCH_2OH$ + CH_3OH. As illustrated in Scheme 3, the overall

Scheme 3. Schematic Illustration of the Mechanism for Ester Hydrogenation

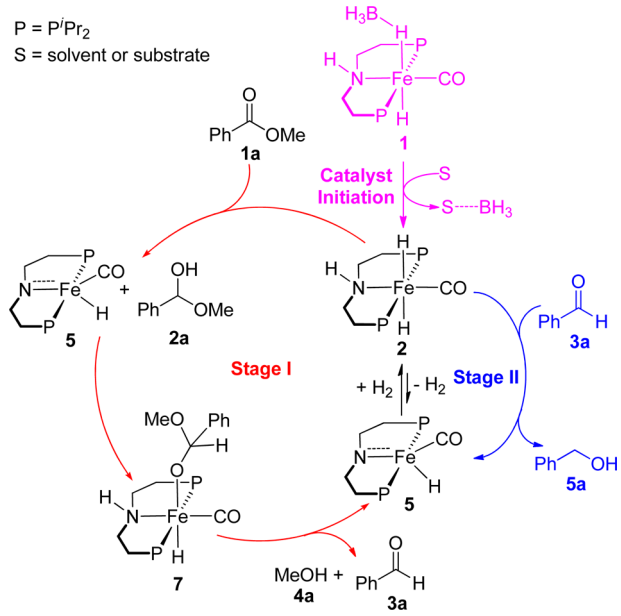

transformation proceeds via two stages: (stage I) transformation of methyl benzoate to benzaldehyde (**3a**) and methanol (**4a**), taking place via hydrogenation of methyl benzoate to a hemiacetal intermediate **2a**, followed by the decomposition of **2a**, and (stage II) hydrogenation of benzaldehyde to benzyl alcohol. Both stages dehydrogenate **2** to **5**. The addition of H_2 to **5** regenerates **2**. For each of the stages, we will discuss the details of the mechanism and highlight the differences between our mechanism and the one proposed by Beller and co-workers.

*3.2.1. Transformation of Methyl Benzoate to Benzaldehyde (**3a**) and Methanol (**4a**) (Stage I).* The detailed mechanism for stage I is depicted in Figure 1A, with energetic results given in Figure 1B and key optimized structures displayed in Figure 2. This stage can be characterized by three processes, including the hydrogenation of methyl benzoate (**1a**) to the hemiacetal intermediate (**2a**), decomposition of **2a** via

dx.doi.org/10.1021/cs501089h | ACS Catal. 2014, 4, 4377−4388

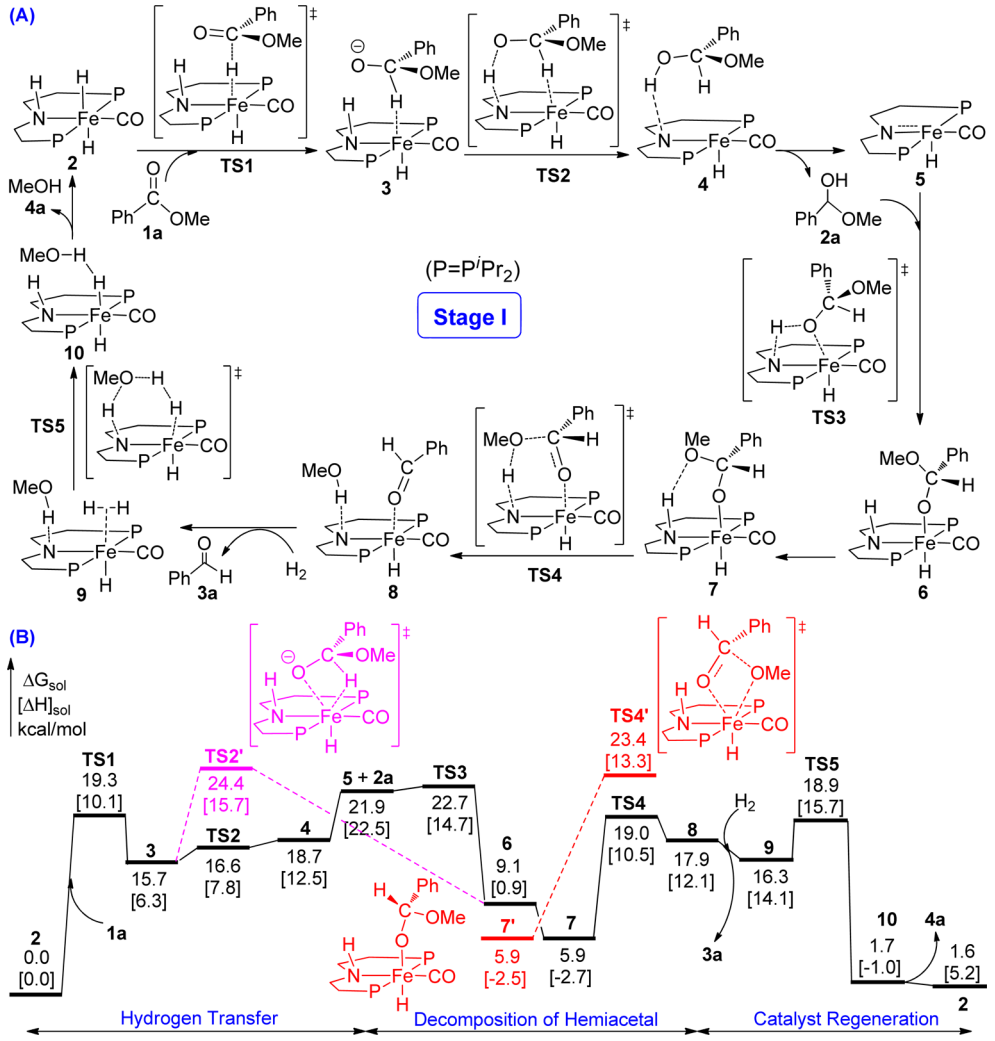

Figure 1. (A) Catalytic mechanism for methyl benzoate (**1a**) to benzaldehyde (**3a**) and methanol (**4a**); and (B) free-energy profile of stage I.

C−O bond cleavage, and H_2 addition to recover the active catalyst.

The hydrogenation of methyl benzoate by **2** to form **4** proceeds via stepwise hydrogen transfers, which is similar to the BDHT (bifunctional double hydrogen transfer) step in Scheme 1, first transferring the Fe−H hydride via **TS1** and then N−H via **TS2**. In comparison, Beller et al. reported a concerted hydrogenation pathway.[15] The difference is minor; first, the different DFT levels of calculations may result in the difference; second, our stepwise pathway can be considered as concerted, because the second hydrogen transfer is very facile, as shown by the small energy difference (3.0 kcal/mol) between **3** and **4**. **TS2** can be optimized in the gas phase, but disappears after corrections of solvation effects and thermal corrections. Complex **4** from the hydrogen transfer step is a weak H-bond complex, as reflected by the atomic distances of N−H (1.920 Å, see Figure S6 in SI). The dissociation of hemiacetal **2a** from **4** costs 3.2 kcal/mol. Note that complex **5** from the dissociation has been recently isolated and characterized by X-ray crystallography.[19] Overall, the hydrogenation of **1a** to **2a** + **5** is thermodynamically unfavorable (by 21.9 kcal/mol), though the kinetic barrier is not high. Thus, a way to improve the performance of the approach could be to tune the catalyst to have better energetics for this process.

The adduct **1a**···BH_3 may exist as a transient intermediate in the system. The binding of BH_3 may potentially facilitate the hydrogen transfer from **2** to **1a**, because the carbonyl carbon becomes more electropositive, favoring hydride transfer, although it reduces the basicity of the carbonyl oxygen, resulting in less favorable proton transfer. Our calculations show that the binding indeed lowers the barrier of the hydride transfer (corresponding to **TS1** step in Figure 2), but the binding does not benefit the overall process of converting **2** + **1a** to **5** + **2a** in Figure 1 (see Figure S3). As suggested above, BH_3 may not accumulate in the system, but rather, it may be converted to B_2H_6 or higher boranes.

Complex **5** has a bifunctional active site (Fe−N) that can activate the O−H bond of **2a** readily via addition, giving **6**. Relative to **2a** + **5**, the addition crosses a barrier of only 0.8 kcal/mol and is exergonic by 12.8 kcal/mol. Complex **6** rearranges to a more stable isomer **7** due to the favorable H-bond interaction of Me−O···H−N (see Figure S6 in SI). Subsequently, the proton transfers from nitrogen to the OMe group, crossing a barrier of 13.1 kcal/mol (**TS4**), resulting in the cleavage of C−OMe bond and a ternary complex **8**.

The pathway from **2** + **1a** to **7** in Figure 1 is essentially similar to the blue pathway (metal−ligand cooperation, MLC) in Scheme 1 reported by us as one of the stages for Ru-catalyzed hydrogenation of carbonates to alcohols (eq 2).[20]

dx.doi.org/10.1021/cs501089h | ACS Catal. 2014, 4, 4377−4388

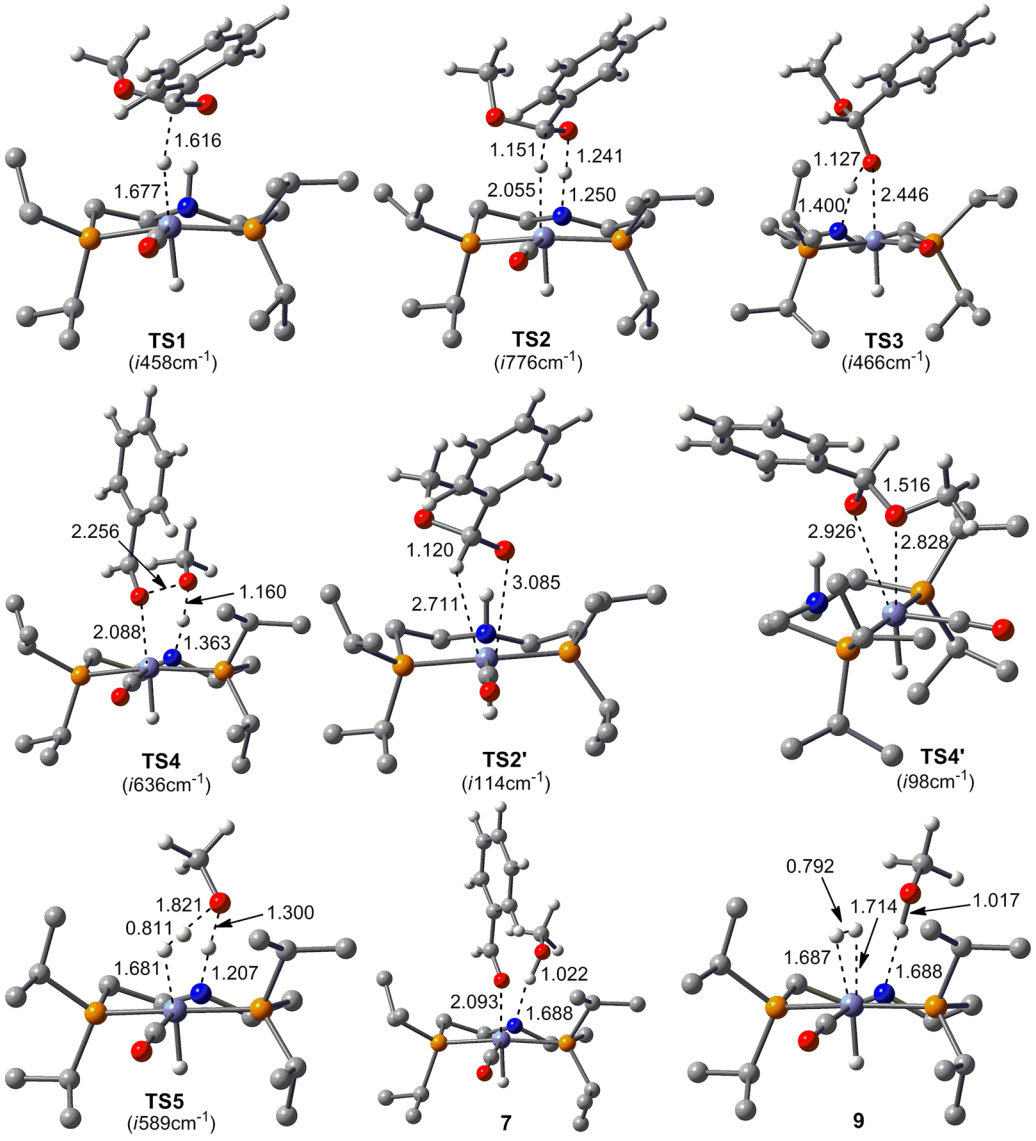

Figure 2. Optimized geometries of the key stationary points labeled in Figure 1, along with the key bond lengths in angstroms. Trivial hydrogen atoms are omitted for clarity. Values in parentheses are imaginary frequencies for transition states.

Yang and Hasanayn reported alternative pathways for the Ru system,[22,23] as shown in green and red in Scheme 1, respectively. Given these studies, we became interested in investigating if these two mechanistic pathways are viable for the present Fe-based catalytic system. Similar to the red pathway, **6** may form directly from **3** through insertion of the carbonyl group into the Fe−H bond via **TS2′**. This pathway avoids formation of a free hemiacetal intermediate **2a**, but is slightly less favorable than our mechanism discussed above; **TS2′** is 1.7 kcal/mol higher than **TS3**. For the cleavage of the C−OMe bond, we also examined two scenarios of the "slippage mechanism"[23] that are analogous to those in Scheme 1. Because the protruding (N−)H in **6**, the TS corresponding to "slippage mechanism I" in Scheme 1 could not be found. Nevertheless, **TS4′** corresponding to "slippage mechanism II" could be located (see Figure 2 for its structure). Because **TS4′** is 4.4 kcal/mol higher than **TS4**, the "slippage mechanism" seems not likely to be operating in the present catalytic system. For the ion-pair dissociation pathway, the dissociation of (MeO)-CHPhO$^-$ from **3** costs 11.9 kcal/mol, which places the dissociation products 4.9 kcal/mol above **TS3**, thus the mechanism for forming **6** is also less favorable than the MLC mechanism.

Beller et al. proposed that the hemiacetal **2a** decomposes to **4a** and **3a** without involving any Fe complex.[15] Figure 3

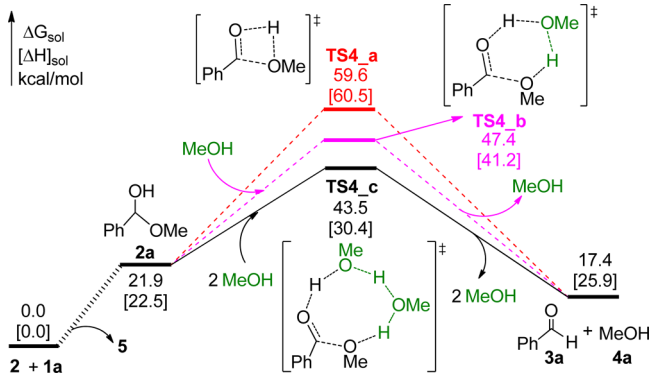

Figure 3. Pathway for the direct decomposition of the hemiacetal intermediate **2a**.

dx.doi.org/10.1021/cs501089h | ACS Catal. 2014, 4, 4377−4388

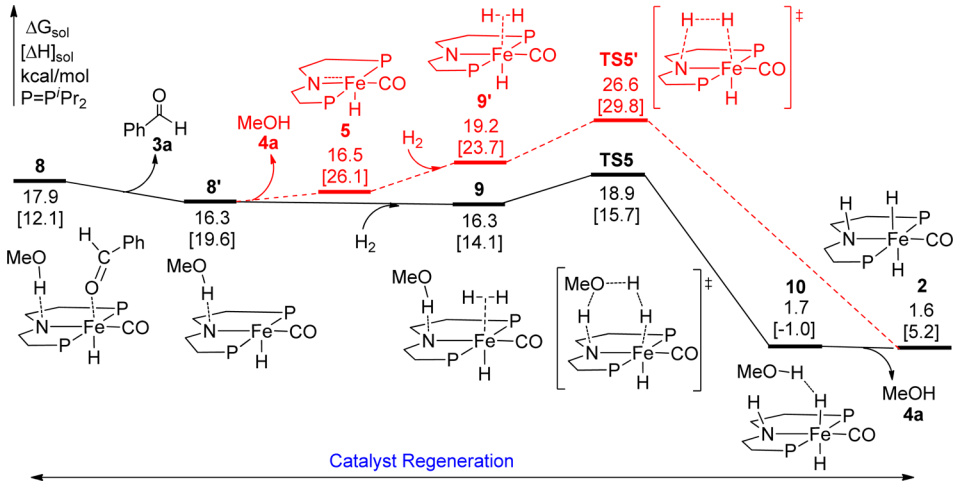

Figure 4. Pathways for catalyst regeneration with or without the assistance of methanol.

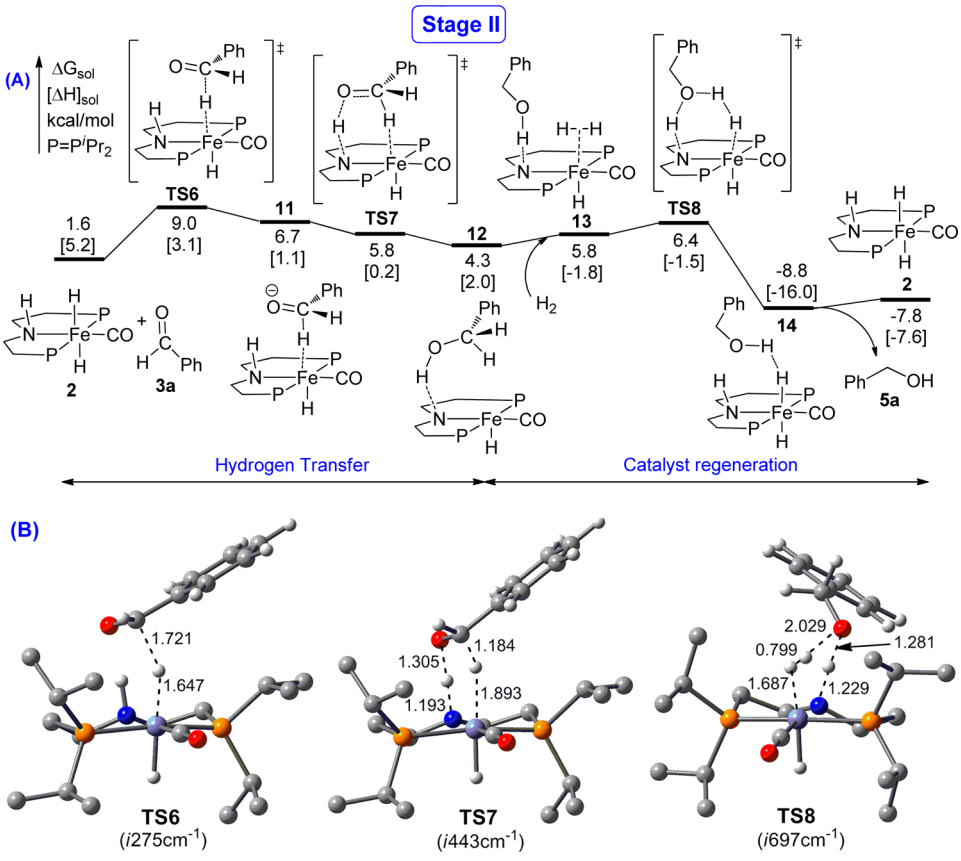

Figure 5. (A) Energy profile for hydrogenation of benzaldehyde (**3a**) to benzyl alcohol **5a** (Stage II); (B) optimized geometries of the key stationary points along with the key bond lengths in angstroms. Trivial hydrogen atoms are omitted for clarity. Values in parentheses are imaginary frequencies for transition states.

summarizes the energetics of different mechanisms. Relative to **2a**, the barrier for direct decomposition of **2a** via **TS4_a** is 37.7 kcal/mol. Using proton shuttles containing one and two methanol molecules lowers the barrier to 25.5 (**TS4_b** relative to **2a** + MeOH) and 21.6 kcal/mol (**TS4_c** relative to **2a** + 2MeOH), respectively. The barrier 21.6 kcal/mol (**TS4_c**) is not high for the decomposition of **2a**. But if projecting **TS4_c** to the starting energy point (**2** + **1a**), the relative energy of **TS4_c** would be 43.5 kcal/mol, which is too high to be viable. By comparison, along the path (from **5** + **2a** to **7**) shown in Figure 1, the addition of **2a** to **5** via **TS3** is almost barrierless and drives the system downhill by 16.0 kcal/mol. In addition, the barrier for cleaving the C−O bond via **TS4** is low (13.1 kcal/mol). Therefore, complex **5** greatly facilitates the decomposition of **2a** to **3a** and **4a**.

Referring to Figure 1, the C−O bond cleavage in **7** via **TS4** leads to complex **8** in which methanol and benzaldehyde molecules are formed, but both weakly interact with **5** through H-bond and coordination, respectively. Figure 4 details the subsequent release of methanol and benzaldehyde and H_2

dx.doi.org/10.1021/cs501089h | ACS Catal. 2014, 4, 4377−4388

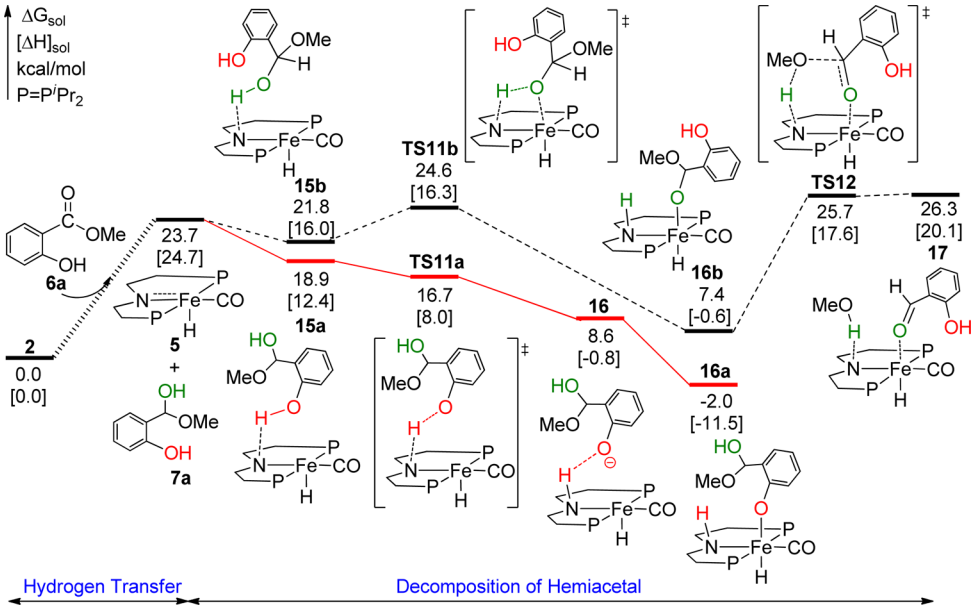

Figure 6. Comparison of the pathway for methyl salicylate (**6a**) reduction to alcohols (in black) to that (in red) of the addition of phenyl OH group to **5** (a side reaction).

addition to regenerate the active catalyst **2**. Along the pathway in black, the methanol moiety stays and acts as a hydrogen transfer shuttle for H_2 addition. The dissociation of benzaldehyde from **8** is slightly exergonic by 1.6 kcal/mol mainly owing to the entropy contribution of the dissociation process. Then the H_2 molecule coordinates to the vacant site of the Fe center, leading to **9**. The H_2 addition aided by the methanol H-transfer shuttle crosses a barrier of only 2.6 kcal/mol (**TS5**), resulting in **10**. Finally, the dissociation of methanol from **10** regenerates the active catalyst **2**. Along the pathway in red, the methanol **4a** is liberated from **8′**, and then complex **5** activates H_2 via **TS5′**. Comparing the two pathways, **TS5** is 7.7 kcal/mol lower than **TS5′**, indicating the methanol proton transfer shuttle facilitates the H_2 activation greatly in the catalyst regeneration. The facilitating effect of a proton shuttle on the proton transfer has also been observed in the H_2-elimination process.[29a]

3.3. Hydrogenation of Benzaldehyde (3a) to Benzyl Alcohol (5a) (Stage II). Benzaldehyde (**3a**) formed in stage I can be further hydrogenated to benzyl alcohol (**5a**). Figure 5 shows the pathway for **3a** hydrogenation, along with the energetic and geometric results. The transformation proceeds via two steps (hydrogenation and catalyst regeneration). The hydrogenation takes place stepwise via crossing **TS6** and then **TS7**. As expected, the barriers for hydrogenation of **3a** through **TS6** and **TS7** (7.4 and 4.2 kcal/mol relative to **2** + **3a**, respectively) are lower than those (19.3 (**TS1**) and 16.6 kcal/mol (**TS2**) relative to **2** + **1a**) for the hydrogenation of ester **1a** in stage I. Complex **12** is the counterpart of **4** in stage I. The catalyst regeneration is accomplished via H_2 addition to **12** to give a dihydrogen complex **13**, followed by crossing **TS8** on route to **14**. Relative to H_2 + **12**, the barrier for the H_2 activation is 2.1 kcal/mol. Finally, the benzyl alcohol **5a** dissociates from **14** to regenerate the active catalyst **2**.

Putting the two stages together, stages I is endergonic by 1.6 kcal/mol and the stage II is exergonic by 9.4 kcal/mol. Overall, the transformation (**1a** + $2H_2$ → **4a** + **5a**) is exergonic by 7.8 kcal/mol, which is the thermodynamic driving force for the transformation. The rate-determining step is the hydrogenation of the ester (**1a**).

3.3. Why the Catalytic System Does Not Work for Methyl Salicylate? In our experimental study,[14] we observed that the catalyst was not able to promote the hydrogenation of methyl salicylate (**6a**). On the basis of mechanistic understanding of the eq 1 reaction, the causes are obvious. As detailed in SI (Figure S7), similar to the hydrogenation of **1a**, a hydrogenation process leads **2** + **6a** to the hemiacetal **7a** + **5** (see Figure 6). Unlike **2a**, **7a** bears two hydroxyl groups, namely, the hemiacetal hydroxyl group (in green) and phenol hydroxyl group (in red). As a result, there is a competition between additions of the two OH groups to the Fe−N active site of **5**. To produce the desired alcohols, the reaction should proceed along the pathway in black, adding the hemiacetal OH group to the active site to finally give **17** (similar to **8** in Figure 1). However, the phenyl OH group is more reactive for the addition (a side reaction); **TS11a** for the addition could be located in terms of electronic energy in the gas phase, but it disappears after the corrections of solvation effect and thermal contributions, thus the addition of the hemiacetal OH group could be downhill straight forwardly. In comparison, the pathway leading **7a** + **5** to **17** crosses high barriers **TS11b** ($\Delta G^{\ddagger}$ = 24.6 kcal/mol) and **TS12** ($\Delta G^{\ddagger}$ = 25.7 kcal/mol). In addition, **16a** is 9.4 and 28.3 kcal/mol more stable than **16b** and **17**. Therefore, the side reaction (addition of the phenol OH group to **5**) is more favorable than the reaction leading to **17** in terms of both kinetics and thermodynamics. Furthermore, **6a** is less reactive than **1a** toward the hydrogenation to their hemiacetal intermediates **7a** and **2a**, respectively; the former is endogonic by 23.7 kcal/mol, while the latter is endogonic by 21.9 kcal/mol. For the subsequent hemiacetal decomposition, **7a** is also more difficult to decompose than **2a**, as reflected by the larger relative energies of **TS11b**/**TS12** (24.6/25.7 kcal/mol) than **TS3**/**TS4** (22.7/19.0 kcal/mol). Taken together, we attribute the failure of the catalyst to promote the hydrogenation of **6a** to (i) the more favorable side reaction of adding the phenol group of **7a**, which deactivates the catalyst, and (ii) the intrinsic inertness of **6a** toward the reduction. Of note is

dx.doi.org/10.1021/cs501089h | ACS Catal. 2014, 4, 4377−4388

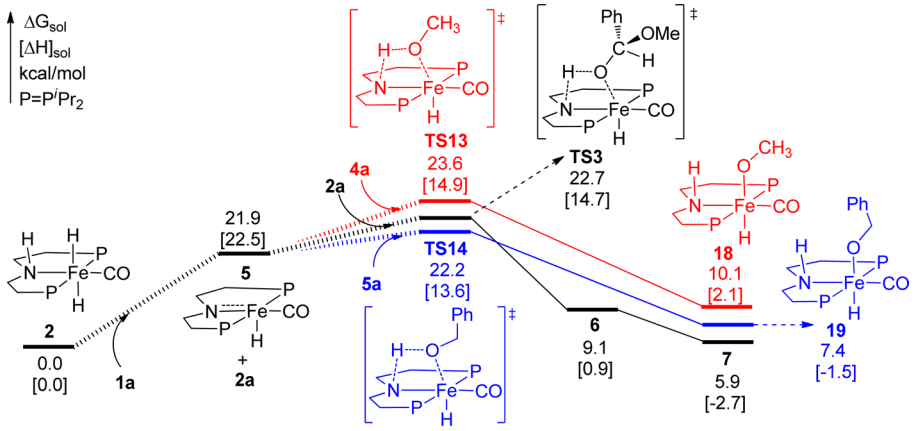

Figure 7. Possible competitive side reactions (blue and red) in the hydrogenation of **1a**.

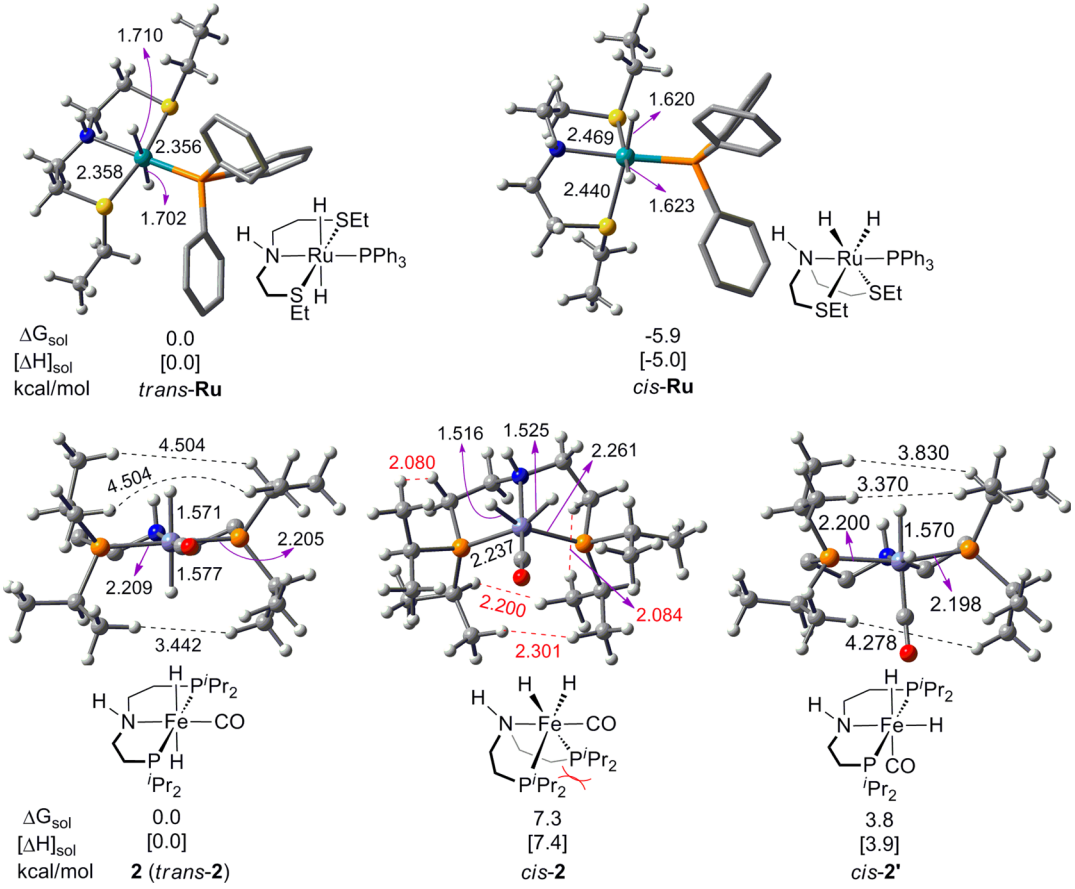

Figure 8. Comparison of stability of *cis* or *trans* isomers of dihydride Ru/Fe complexes. Key bond lengths are in angstroms. Trivial hydrogen atoms are omitted for clarity.

that the phenol group of **6a** can also add to the Fe−N active site but is less favorable than the addition of the phenol hydroxyl group of **7a** (see SI).

To corroborate the above understanding on the failed reaction for **6a**, we further considered similar side reactions that may occur to the reaction shown in eq 1, because the alcohol products (**4a** or **5a**) may compete with the hemiacetal **2a** for adding to the Fe−N site of **5**. Figure 7 compares the main reaction with these side reactions. Unlike **6a**, the addition of OH groups of **4a** and **5a** (leading to **18** and **19**, respectively) is thermodynamically less favorable than that of **2a** (leading to **7** in the main reaction). Although **TS13** and **TS14** are comparable with **TS3** in energy, the thermodynamic preference of **7** over **18** and **19** drives the reactions to **7**, because the reverse barriers from **18** and **19** to **TS13** and **TS14** are not high, being 13.5 and 14.8 kcal/mol, respectively. Thus, these side reactions cannot suppress the main reaction, supporting our rationale on why the catalyst was not able to catalyze the hydrogenation of **6a**. Because the rationalization invokes **5** to participate in the hemiacetal decomposition, the reasonable explanation gives support to our mechanism for the hemiacetal decomposition involving **5**.

dx.doi.org/10.1021/cs501089h | *ACS Catal.* 2014, 4, 4377−4388

4. FURTHER DISCUSSION ON THE ACTIVE SPECIES 2

The active species **2** has analogs in ruthenium complexes such as **Ru** in Figure 8. It is known that **Ru** has two isomers (i.e., *trans*-**Ru** and *cis*-**Ru**).[38] We predicted that *trans*-**Ru** is 5.9 kcal/mol less stable than *cis*-**Ru**, which can be attributed to the destabilization in *trans*-**Ru** when placing two strongly *trans* influencing hydride ligands opposite to each other. As an additional evidence, the two Ru−H bonds (1.710/1.702 Å) in *trans*-**Ru** are longer than those (1.620/1.623 Å) in *cis*-**Ru**. In contrast, *trans*-**2** is 7.3 kcal/mol more stable than *cis*-**2**, even though the *trans* influence remains a factor; the two Fe−H bonds (1.571/1.577 Å) in *trans*-**2** are longer than those (1.516/1.525 Å) in *cis*-**2**. Geometric comparison of the two isomers of **2** reveals that the steric hindrance between the two P^iPr_2 groups of *cis*-**2** is the origin for reversing the order of stability. In *cis*-**Ru**, the −SEt substituent is not bulky enough to cause severe steric hindrance. To corroborate this, we considered the *trans* and *cis* isomers of another Ru complex that is similar to **2** but with a replacement of Fe with Ru (see Figure S5). Similar to **2**, the *trans* isomer of the Ru complex is 6.9 kcal/mol more stable than its *cis* isomer. It is interesting to point out that *trans*-dihydride complexes are typically less stable than the corresponding *cis*-dihydride complexes. However, as demonstrated in this work, the steric hindrance within the ligand could override the *trans* effect so that the *trans* isomers can become more stable. This proves to be critical to the success of the hydrogenation reactions, because in *trans*-**2**, the hydride that is transferred to **1a** (via **TS1**) is being placed opposite to a strongly *trans*-influencing hydride ligand, which results in more facile hydride transfer.

We further consider a third isomer of **2**, namely, *cis*-**2′**. Because of the steric hindrance of CO ligand with its nearby P^iPr_2 groups, *cis*-**2′** is 3.8 kcal/mol less stable than *trans*-**2**. Furthermore, although CO is also a ligand with strong *trans* effect (the bond length of Fe−H *trans* to CO, 1.570 Å, is comparable with those in **2**), the barrier (26.7 kcal/mol, **TS1′** in Figure S4) for hydride transfer from *cis*-**2′** to **1a** is higher than **TS1** (19.3 kcal/mol), because the CO ligand in *cis*-**2′** pushes the two P^iPr_2 groups closer to the *trans*-hydride ligand, creating a sterically more demanding environment for hydride transfer.

5. CONCLUSIONS

In summary, we have performed DFT computations to understand the whole catalytic process of the ester hydrogenation (i.e., methyl benzoate to methanol and benzyl alcohol) promoted by the well-defined Fe-PNP pincer complex (**1**). The catalytic process includes activation of precatalyst **1** to an active catalyst **2**, **2**-catalyzed hydrogenation of methyl benzoate to benzaldehyde and methanol as well as hydrogenation of benzaldehyde to benzyl alcohol, and catalyst regeneration via H_2 addition to the dehydrogenated **2** (i.e., complex **5**). The overall transformation of $PhCO_2CH_3 + 2H_2 \rightarrow PhCH_2OH + CH_3OH$ is exergonic by 7.8 kcal/mol. Without an additive (original experimental condition), various catalyst initiation processes were explored, which cross 21.0−25.0 kcal/mol barriers and are endergonic by 11−26 kcal/mol. The transformation of $PhCO_2CH_3 + H_2 \rightarrow PhCHO + CH_3OH$ proceeds via three sequential steps including hydrogenation of methyl benzoate to a hemiacetal intermediate **2a**, decomposition of **2a** to benzaldehyde and methanol, and H_2 addition to recovery the active catalyst. Two other pathways for the transformation of $PhCO_2CH_3 + H_2 \rightarrow PhCHO + CH_3OH$ were examined and were determined to be less feasible. The Fe-complex **5** was found capable of greatly facilitating the decomposition of **2a**. On the basis of the understanding of the representative reaction, we attributed the failure of **2** to catalyze the hydrogenation of methyl salicylate to the lower reactivity of the ester itself toward the transformation and a very facile side-reaction, namely, the addition of the phenol OH group of hemiacetal intermediate to the Fe−N active site of **5**.

Because the catalyst initiation (without the aid of additive) is energetically unfavorable, we proposed to add a Lewis base (e.g., NR_3 (R = Me or Et) and PR_3 (R = ^{n}Bu or ^{t}Bu) to promote the activation of precatalyst (**1**). Our computations show the formation of a Lewis base/acid complex (BH_3−NR_3/PR_3) can indeed greatly facilitate the precatalyst activation kinetically and thermodynamically. Consistent with this prediction, experimental data on the hydrogenation of methyl benzoate show that the addition of NEt_3 to the catalytic system doubled the yield for benzyl alcohol, when compared to the case without adding NEt_3. More detailed experimental study of this strategy is currently in progress.

The catalytically active species **2** contains two hydride ligands that are *trans* to each other. The strongly *trans*-influencing hydride facilitates the transfer of the other hydride from **2** to **1a**. The geometric isomer *cis*-**2**, in which two hydrides are *cis* to each and the pincer ligand adopts a *fac* configuration, is less stable than **2** (*trans*-**2**), because the *cis* isomer suffers from sever steric repulsion from two P^iPr groups.

■ ASSOCIATED CONTENT

Supporting Information

The following files are available free of charge on the ACS Publications website at DOI: 10.1021/cs501089h.

Additional computational results, total energies, and Cartesian coordinates of all optimized structures (PDF).

■ AUTHOR INFORMATION

Corresponding Authors

*E-mail: zxwang@ucas.ac.cn (Z.X.W.).

*E-mail: hairong.guan@uc.edu (H.G.).

Notes

The authors declare no competing financial interest.

■ ACKNOWLEDGMENTS

We acknowledge the financial support from National Natural Science Foundation of China (Nos. 21173263 and 21373216), the Procter & Gamble Company, and the Alfred P. Sloan Foundation (research fellowship to H.G.).

■ REFERENCES

(1) (a) Dub, P. A.; Ikariya, T. *ACS Catal.* **2012**, *2*, 1718−1741. (b) Saudan, L. A. In *Sustainable Catalysis*; Dunn, P. J., Hii, K. K., Krische, M. J., Williams, M. T., Eds.; Wiley: Hoboken, NJ, 2013; pp 37−61.

(2) (a) Rylander, P. N. *Catalytic Hydrogenation in Organic Syntheses*; Academic Press: New York, 1979. (b) Nishimura, S. *Handbook of Heterogeneous Catalytic Hydrogenation for Organic Synthesis*; Wiley: New York, 2001. (c) Clarke, M. L.; Roff, G. J. In *Handbook of Homogeneous Hydrogenation*; Johannes, G. d. V., Elsevier, C. J., Eds.; Wiley-VCH: Weinheim , 2007. (d) Andersson , P. G. ; Munslo, I. J. *Modern Reduction Methods*; Wiley: New York, 2008 .

(3) *Analysis of the natural fatty alcohol market in Southeast Asia*; Subscription No. P710-01; Frost & Sullivan: Singapore, 2013.

(4) (a) Greeves, N. In *Comprehensive organic synthesis: selectivity, strategy, and efficiency in modern organic chemistry*, 1st ed.; Trost, B. M., Fleming, I., Eds.; Pergamon Press: Oxford, NY, 1991; Vol. *8*, pp 1 − 25. (b) Seyden-Penne , J. *Reductions by the alumino- and borohydrides in organic synthesis*, 2nd ed.; Wiley-VCH: New York, 1997.
(5) (a) Rieke, R. D.; Thakur, D. S.; Roberts, B. D.; White, G. T. *J. Am. Oil Chem. Soc.* **1997**, *74*, 333−339. (b) Pouilloux, Y.; Autin, F.; Barrault, J. *Catal. Today* **2000**, *63*, 87−100. and references therein. (c) Adkins, H. *Org. React.* **1954**, *8*, 1−27.
(6) (a) Werkmeister, S.; Junge, K.; Beller, M. *Org. Process Res. Dev.* **2014**, *18*, 289−302. (b) Clarke, M. L. *Catal. Sci. Technol.* **2012**, *2*, 2418−2423.
(7) Teunissen, H. T.; Elsevier, C. J. *Chem. Commun.* **1997**, 667−668.
(8) Grey, R. A.; Pez, G. P.; Wallo, A. *J. Am. Chem. Soc.* **1981**, *103*, 7536−7542.
(9) (a) Nomura, K.; Ogura, H.; Imanishi, Y. *J. Mol. Catal. A: Chem.* **2002**, *178*, 105−114. (b) Teunissen, H. T.; Elsevier, C. J. *Chem. Commun.* **1998**, 1367−1368.
(10) Zhang, J.; Leitus, G.; Ben-David, Y.; Milstein, D. *Angew. Chem., Int. Ed.* **2006**, *45*, 1113−1115.
(11) (a) Saudan, L.; Dupau, P. ; Riedhauser, J.-J. ; Wyss, P. (Firmenich SA), Patent WO WO2006106483 and WO 2006106484, October 12, 2006. (b) Saudan, L. A.; Saudan, C. M.; Debieux, C.; Wyss, P. *Angew. Chem., Int. Ed.* **2007**, *46*, 7473−7476.
(12) (a) Liu, C.; Xie, J.-H.; Li, Y.-L.; Chen, J.-Q.; Zhou, Q.-L. *Angew. Chem., Int. Ed.* **2013**, *52*, 593−596. (b) Spasyuk, D.; Smith, S.; Gusev, D. G. *Angew. Chem., Int. Ed.* **2013**, *52*, 2538−2542. (c) Ziebart, C.; Jackstell, R.; Beller, M. *ChemCatChem* **2013**, *5*, 3228−3231. (d) Westerhaus, F. A.; Wendt, B.; Dumrath, A.; Wienhöfer, G.; Junge, K.; Beller, M. *ChemSusChem* **2013**, *6*, 1001−1005. (e) Junge, K.; Wendt, B.; Westerhaus, F. A.; Spannenberg, A.; Jiao, H.; Beller, M. *Chem.—Eur. J.* **2012**, *18*, 9011−9018. (f) Spasyuk, D.; Gusev, D. G. *Organometallics* **2012**, *31*, 5239−5242. (g) Carpenter, I.; Eckelmann, S. C.; Kuntz, M. T.; Fuentes, J. A.; France, M. B.; Clark, M. L. *Dalton Trans.* **2012**, *41*, 10136−10140. (h) Spasyuk, D.; Smith, S.; Gusev, D. G. *Angew. Chem., Int. Ed.* **2012**, *51*, 2772−2775. (i) Kuriyama, W.; Matsumoto, T.; Ogata, O.; Ino, Y.; Aoki, K.; Tanaka, S.; Ishida, K.; Kobayashi, T.; Sayo, N.; Saito, T. *Org. ProcessRes. Dev* **2012**, *16*, 166−171. (j) Dub, P. A.; Ikariya, T. *ACS Catal.* **2012**, *2*, 1718−1741. (k) Clarke, M. L. *Catal. Sci. Technol.* **2012**, *2*, 2418−2423. (l) Fogler, E.; Balaraman, E.; Ben-David, Y.; Leitus, G.; Shimon, L.J. W.; Milstein, D. *Organometallics* **2011**, *30*, 3826−3833. (m) Zhang, J.; Balaraman, E.; Leitus, G.; Milstein, D. *Organometallics* **2011**, *30*, 5716−5724. (n) Ito, M.; Ootsuka, T.; Watari, R.; Shiibashi, A.; Himizu, A.; Ikariya, T. *J. Am. Chem. Soc.* **2011**, *133*, 4240−4242. (o) Touge, T.; Hakamata, T.; Nara, H.; Kobayashi, T.; Sayo, N.; Saito, T.; Kayaki, Y.; Ikariya, T. *J. Am. Chem. Soc.* **2011**, *133*, 14960−14963. (p) Sun, Y.; Koehler, C.; Tan, R.; Annibale, V. T.; Song, D. *Chem.Commun.* **2011**, *47*, 8349−8351. (q) O, W. W. N.; Lough, A. J.; Morris, R. H. *Chem. Commun.* **2010**, *46*, 8240−8242. (r) Takebayashi, S.; Bergens, S. H. *Organometallics* **2009**, *28*, 2349−2351. (s) Kuriyama, W.; Ino, Y.; Ogata, O.; Sayo, N.; Saito, T. *Adv. Synth.Catal.* **2010**, *352*, 92−96. (t) Chen, T.; Li, H.; Qu, S.; Zheng, B.; He, L.; Lai, Z.; Wang, Z.-X.; Huang, K.-W. *Organometallics* **2014**, *33*, 4152−4155. (u) O, W. W. N.; Morris, R. H. *ACS Catal.* **2013**, *3*, 32−40.
(13) Zell, T.; Ben-David, Y.; Milstein, D. *Angew. Chem., Int. Ed.* **2014**, *53*, 4685−4689.
(14) Chakraborty, S.; Dai, H.; Bhattacharya, P.; Fairweather, N. T.; Gibson, M. S.; Krause, J. A.; Guan, H. *J. Am. Chem. Soc.* **2014**, *136*, 7869−7872.
(15) Werkmeister, S.; Junge, K.; Wendt, B.; Alberico, E.; Jiao, H.; Baumann, W.; Junge, H.; Gallou, F.; Beller, M. *Angew. Chem., Int. Ed.* **2014**, *53*, 8722−8726.
(16) (a) Alberico, E.; Sponholz, P.; Cordes, C.; Nielsen, M.; Drexler, H.-J.; Baumann, W.; Junge, H.; Beller, M. *Angew. Chem., Int. Ed.* **2013**, *52*, 14162−14166. (b) Chakraborty, S.; Lagaditis, P. O.; Förster, M.; Bielinski, E. A.; Hazari, N.; Holthausen, M. C.; Jones, W. D.; Schneider, S. *ACS Catal.* **2014**, *4*, 3994−4003.
(17) Bielinski, E. A.; Lagaditis, P. O.; Zhang, Y.; Mercado, B. Q.; Würtele, C.; Bernskoetter, W. H.; Hazari, N.; Schneider, S. *J. Am. Chem. Soc.* **2014**, *136*, 10234−10237.
(18) Lagaditis, P. O.; Sues, P. E.; Sonnenberg, J. F.; Wan, K. Y.; Lough, A. J.; Morris, R. H. *J. Am. Chem. Soc.* **2014**, *136*, 1367−1380.
(19) Chakraborty, S.; Brennessel, W. W.; Jones, W. D. *J. Am. Chem. Soc.* **2014**, *136*, 8564−8567.
(20) Li, H.; Wen, M.; Wang, Z. X. *Inorg. Chem.* **2012**, *51*, 5716−5727.
(21) Balaraman, E.; Gunanathan, C.; Zhang, J.; Shimon, L. J. W.; Milstein, D. *Nat. Chem.* **2011**, *3*, 609−614.
(22) Yang, X. *ACS Catal.* **2012**, *2*, 964−970.
(23) (a) Hasanayn, F.; Baroudi, A. *Organometallics* **2013**, *32*, 2493−2496. (b) Hasanayn, F.; Baroudi, A.; Bengali, A. A.; Goldman, A. S. *Organometallics* **2013**, *32*, 6969−6985.
(24) (a) Lee, C. T.; Yang, W. T.; Parr, R. G. *Phys. Rev. B* **1988**, *37*, 785−789. (b) Miehlich, B.; Savin, A.; Stoll, H.; Preuss, H. *Chem. Phys. Lett.* **1989**, *157*, 200−206. (c) Stephens, P. J.; Devlin, F. J.; Chabalowski, C. F.; Frisch, M. J. *J. Phys. Chem.* **1994**, *98*, 11623−11627.
(25) (a) Gordon, M. S. *Chem. Phys. Lett.* **1980**, *76*, 163−168. (b) Harihara, Pc; Pople, J. A. *Mol. Phys.* **1974**, *27*, 209−214. (c) Harihara, Pc; Pople, J. A. *Theor. Chem. Acc.* **1973**, *28*, 213−222. (d) Hehre, W. J.; Ditchfield, R.; Pople, J. A. *J. Chem. Phys.* **1972**, *56*, 2257−2261. (e) Ditchfield, R.; Hehre, W. J.; Pople, J. A. *J. Chem. Phys.* **1971**, *54*, 724−728.
(26) (a) Kulkarni, A. D.; Truhlar, D. G. *J. Chem. Theory Comput.* **2011**, *7*, 2325−2332. (b) Sliwa, P.; Handzlik, J. *Chem. Phys. Lett.* **2010**, *493*, 273−278. (c) Zhao, Y.; Truhlar, D. G. *J. Chem. Theory Comput.* **2009**, *5*, 324−333. (d) Zhao, Y.; Truhlar, D. G. *Acc. Chem. Res.* **2008**, *41*, 157−167.
(27) (a) Francl, M. M.; Pietro, W. J.; Hehre, W. J.; Binkley, J. S.; Gordon, M. S.; DeFrees, D. J.; Pople, J. A. *J. Chem. Phys.* **1982**, *77*, 3654−3665. (b) Krishnan, R.; Binkley, J. S.; Seeger, R.; Pople, J. A. *J. Chem. Phys.* **1980**, *72*, 650−654. (c) Wachters, A. J. H. *J. Chem. Phys.* **1970**, *52*, 1033−1036. (d) Hay, P. J. *J. Chem. Phys.* **1977**, *66*, 4377−4384. (e) Raghavachari, K.; Trucks, G. W. *J. Chem. Phys.* **1989**, *91*, 1062−1065. (f) Binning, R. C.; Curtiss, L. A. *J. Comput. Chem.* **1990**, *11*, 1206−1216. (g) McGrath, M. P.; Radom, L. *J. Chem. Phys.* **1991**, *94*, 511−516. (h) Clark, T.; Chandrasekhar, J.; Spitznagel, G. W.; Schleyer, P. V. R. *J. Comput. Chem.* **1983**, *4*, 294−301. (i) Frisch, M. J.; Pople, J. A.; Binkley, J. S. *J. Chem. Phys.* **1984**, *80*, 3265−3269.
(28) Marenich, A. V.; Cramer, C. J.; Truhlar, D. G. *J. Phys. Chem. B* **2009**, *113*, 6378−6396.
(29) (a) Liu, P.; Xu, X.; Dong, X.; Keitz, B. K.; Herbert, M. B.; Grubbs, R. H.; Houk, K. N. *J. Am. Chem. Soc.* **2012**, *134*, 1464−1467. (b) Giri, R.; Lan, Y.; Liu, P.; Houk, K. N.; Yu, J.-Q. *J. Am. Chem. Soc.* **2012**, *134*, 14118−14126. (c) Herbert, M. B.; Lan, Y.; Keitz, B. K.; Liu, P.; Endo, K.; Day, M. W.; Houk, K. N.; Grubbs, R. H. *J. Am. Chem. Soc.* **2012**, *134*, 7861−7866. (d) Tang, S.-Y.; Guo, Q.-X.; Fu, Y. *Chem.—Eur. J.* **2011**, *17*, 13866−13876. (e) Qu, S.; Dang, Y.; Wen, M.; Wang, Z.-X. *Chem.—Eur. J.* **2013**, *19*, 3827−3832. (f) Ariafard, A.; Asadollah, E.; Ostadebrahim, M.; Rajabi, N. A.; Yates, B. F. *J. Am. Chem. Soc.* **2012**, *134*, 16882−16890. (g) Lin, M.; Kang, G.-Y.; Guo, Y.-A.; Yu, Z.-X. *J. Am. Chem. Soc.* **2012**, *134*, 398−405. (h) Yeom, H.-S.; Koo, J.; Park, H.-S.; Wang, Y.; Liang, Y.; Yu, Z.-X.; Shin, S. *J. Am. Chem. Soc.* **2012**, *134*, 208−211.
(30) Huang, D.; Makhlynets, O. V.; Tan, L. L.; Lee, S. C.; Rybak-Akimova, E. V.; Holm, R. H. *Proc. Natl. Acad. Sci. U.S.A.* **2011**, *108*, 1222−1227.
(31) Liang, Y.; Liu, S.; Xia, Y.; Li, Y.; Yu, Z.-X. *Chem.—Eur. J.* **2008**, *14*, 4361−4373.
(32) Martin, R. L.; Hay, P. J.; Pratt, L. R. *J. Phys. Chem. A* **1998**, *102*, 3565−3573.
(33) (a) Qu, S.; Dang, Y.; Song, C.; Wen, M.; Huang, K. W.; Wang, Z. X. *J. Am. Chem. Soc.* **2014**, *136*, 4974−4991. (b) Wen, M.; Huang, F.; Lu, G.; Wang, Z.-X. *Inorg. Chem.* **2013**, *52*, 12098−12107. (c) Li, H.; Wen, M.; Wang, Z. X. *Inorg. Chem.* **2012**, *51*, 5716−5727. (d) Li,

H.; Jiang, J.; Lu, G.; Huang, F.; Wang, Z.-X. *Organometallics* **2011**, *30*, 3131−3141.
(34) Frisch, M. J.; Trucks, G. W.; Schlegel, H. B.; Scuseria, G. E.; Robb, M. A.; Cheeseman, J. R.; Scalmani, G.; Barone, V.; Mennucci, B.; Petersson, G. A.; Nakatsuji, H.; Caricato, M.; Li, X.; Hratchian, H. P.; Izmaylov, A. F.; Bloino, J.; Zheng, G.; Sonnenberg, J. L.; Hada, M.; Ehara, M.; Toyota, K.; Fukuda, R.; Hasegawa, J.; Ishida, M.; Nakajima, T.; Honda, Y.; Kitao, O.; Nakai, H.; Vreven, T.; Montgomery, J. A., Jr.; Peralta, J. E.; Ogliaro, F.; Bearpark, M.; Heyd, J. J.; Brothers, E.; Kudin, K. N.; Staroverov, V. N.; Kobayashi, R.; Normand, J.; Raghavachari, K.; Rendell, A.; Burant, J. C.; Iyengar, S. S.; Tomasi, J.; Cossi, M.; Rega, N.; Millam, J. M.; Klene, M.; Knox, J. E.; Cross, J. B.; Bakken, V.; Adamo, C.; Jaramillo, J.; Gomperts, R.; Stratmann, R. E.; Yazyev, O.; Austin, A. J.; Cammi, R.; Pomelli, C.; Ochterski, J. W.; Martin, R. L.; Morokuma, K.; Zakrzewski, V. G.; Voth, G. A.; Salvador, P.; Dannenberg, J. J.; Dapprich, S.; Daniels, A. D.; Farkas, O.; Foresman, J. B.; Ortiz, J. V.; Cioslowski, J.; Fox, D. J. *Gaussian 09*, revision A.01; Gaussian, Inc. : Wallingford, CT, 2009.
(35) Greenwood , N. N. ; Earnshaw , A. *Chemistry of the Elements*, 2nd ed.; Elsevier/Butterworth-Heinemann: New York, 1997 .
(36) (a) Dobereiner, G. E.; Crabtree, R. H. *Chem. Rev.* **2009**, *110*, 681−703. (b) Choi, J.; MacArthur, A. H.; Brookhart, M.; Goldman, A. S. *Chem. Rev.* **2011**, *111*, 1761−1779. (c) Li, H.; Wang, Z. *Sci. China-Chem.* **2012**, *55*, 1991−2008. (d) Li, H.; Lu, G.; Jiang, J.; Huang, F.; Wang, Z.-X. *Organometallics* **2011**, *30*, 2349−2363. (e) Li, H.; Wang, X.; Huang, F.; Lu, G.; Jiang, J.; Wang, Z.-X. *Organometallics* **2011**, *30*, 5233−5247. (f) Li, H.; Wang, X.; Wen, M.; Wang, Z.-X. *Eur. J. Inorg. Chem.* **2012**, *2012*, 5011−5020.
(37) In our previous report (ref 14), we showed no catalytic activity of **1** at 60° C. It was likely due to a deteriorated batch of catalyst.
(38) Spasyuk, D.; Smith, S.; Gusev, D. G. *Angew. Chem., Int. Ed.* **2013**, *52*, 2538−2542.